

1
2
3
4
5
6
7
8
9
10
11
12
13
14
15
16
17
18
19
20
21
22
23
24
25
26
27
28
29
30
31
32
33

Human genetic analyses of organelles highlight the nucleus, but not the mitochondrion, in age-related trait heritability

Rahul Gupta^{1,2,3}, Konrad J. Karczewski^{2,3}, Daniel Howrigan^{2,3}, Benjamin M. Neale^{2,3,*}, Vamsi K. Mootha^{1,2,*}

¹ Howard Hughes Medical Institute and Department of Molecular Biology, Massachusetts General Hospital, Boston, MA 02114

² Broad Institute of MIT and Harvard, Cambridge, MA 02142

³ Analytic and Translational Genetics Unit, Center for Genomic Medicine, Massachusetts General Hospital, Boston, MA 02114, USA

*Corresponding authors: bneale@broadinstitute.org (B.M.N.), vamsi@hms.harvard.edu (V.K.M.)

Keywords: mitochondria, nucleus, aging, oxidative phosphorylation, OXPHOS, transcription factor, zinc finger, KRAB domain, gene regulation, UK Biobank, constraint, dominance, haplosufficiency, haplosufficient, PPARGC1A, ESRRA, TFAM

34 **Abstract**

35 Most age-related human diseases are accompanied by a decline in cellular organelle integrity, including
36 impaired lysosomal proteostasis and defective mitochondrial oxidative phosphorylation. An open
37 question, however, is the degree to which inherited variation impacting each organelle contributes to age-
38 related disease pathogenesis. Here, we evaluate if organelle-relevant loci confer greater-than-expected
39 age-related disease risk. As mitochondrial dysfunction is a “hallmark” of aging, we begin by assessing
40 nuclear and mitochondrial DNA loci relevant to mitochondria and surprisingly observe a lack of
41 enrichment across 24 age-related traits. Within nine other organelles, we find no enrichment with one
42 exception: the nucleus, where enrichment emanates from nuclear transcription factors. In agreement, we
43 find that genes encoding several organelles tend to be “haplosufficient,” while we observe strong
44 purifying selection against protein-truncating variants impacting the nucleus. Our work identifies common
45 variation near transcription factors as having outsize influence on age-related trait risk, motivating future
46 efforts to determine if and how this variation contributes to age-related organelle deterioration.

47

48 **Introduction**

49 The global burden of age-related diseases such as type 2 diabetes (T2D), Parkinson's disease (PD), and
50 cardiovascular disease (CVD) has been steadily rising due in part to a progressively aging population. These
51 diseases are often highly heritable¹. Genome-wide association studies (GWAS) have led to the discovery
52 of thousands of robust associations with common genetic variants², implicating a complex genetic
53 architecture as underlying much of the heritable risk. These loci hold the potential to reveal underlying
54 mechanisms of disease and spotlight targetable pathways.

55 Aging has been associated with dysfunction in many cellular organelles³. Dysregulation of autophagic
56 proteostasis, for which the lysosome is central, has been implicated in myriad age-related disorders
57 including neurodegeneration, heart disease, and aging itself⁴, and mouse models deficient for autophagy
58 in the central nervous system show neurodegeneration^{5,6}. Endoplasmic reticular (ER) stress has been
59 invoked as central to metabolic syndrome and insulin resistance in type 2 diabetes⁷. Disruption in the
60 nucleus through increased gene regulatory noise from epigenetic alterations³ and elevated nuclear
61 envelope "leakiness"⁸ has been implicated in aging. Dysfunction in the mitochondria has even been
62 invoked as a "hallmark" of aging³ and has been nominated as a driver of virtually all common age-
63 associated diseases. In particular, deficits in mitochondrial oxidative phosphorylation (OXPHOS) have
64 been observed in aging and age-related diseases as evidenced by *in vivo* ³¹P-NMR measures^{9,10}, enzymatic
65 activity¹¹⁻¹⁷ in biopsy material, accumulation of somatic mitochondrial DNA (mtDNA) mutations¹⁸⁻²⁰, and
66 a decline in mtDNA copy number (mtCN)²¹.

67 Given that a decline in organelle function is observed in age-related disease, a natural question is whether
68 inherited variation in loci relevant for organelles are enriched for age-related disease risk. In the present
69 study, we use a human genetics approach to assess common variation in loci relevant to the function of
70 10 cellular organelles. We begin with a deliberate focus on mitochondria given the depth of literature
71 linking it to age-related disease. As mitochondria-localizing protein products from ~1100 nuclear DNA
72 (nucDNA)-encoded genes²² and 13 mtDNA-encoded genes are critical for proper OXPHOS homeostasis²³,
73 we test both nucDNA and mtDNA loci relevant for mitochondrial function in 24 different age-related
74 diseases and traits. We hypothesized that heritability for common, age-related traits would be
75 overrepresented among mitochondria-relevant loci, namely variants near genes encoding the organelle's
76 proteome or loci associated with quantitative readouts of mitochondrial function.

77 To our surprise, we find no evidence of enrichment for genome-wide association signal in mitochondria-
78 relevant loci across any of our analyses. Further, of ten tested organelles, only the nucleus shows
79 enrichment among many age-associated traits, with the signal emanating from the transcription factors.
80 Further analysis shows that genes encoding the mitochondrial proteome tend to be tolerant to
81 heterozygous predicted loss-of-function (pLoF) variation and thus are surprisingly "haplosufficient,"
82 whereas nuclear transcription factors are especially sensitive to gene dosage and are often
83 "haploinsufficient". Thus, we highlight variation influencing gene-regulatory pathways, rather than
84 organelle physiology, in the inherited risk of common age-associated diseases.

85 **Results**

86 **Age-related diseases and traits show diverse genetic architectures**

87 To systematically define age-related diseases, we turned to recently published epidemiological data from
88 the United Kingdom (U.K.)²⁴ in order to match the U.K. Biobank (UKB)²⁵ cohort. We prioritized traits whose
89 prevalence increased as a function of age (**Methods**) and were represented in UKB
90 (https://github.com/Nealelab/UK_Biobank_GWAS) and/or had available published GWAS meta-
91 analyses²⁶⁻³⁵ (**Figure 1A, Supplementary note**). We used SNP heritability estimates from stratified linkage
92 disequilibrium score regression (S-LDSC, <https://github.com/bulik/ldsc>)³⁶ to ensure that our selected traits
93 were sufficiently heritable (**Methods, Supplementary note**). We then computed pairwise genetic

94 correlations between the age-associated traits to compare their respective genetic architectures (**Figure**
 95 **1B**, **Table S2**, **Methods**). As expected we find a highly correlated module of primarily cardiometabolic
 96 traits with high density lipoprotein (HDL) showing anti-correlation³⁷. Interestingly, several other traits
 97 (gastroesophageal reflux disease (GERD), osteoarthritis) showed moderate correlation to the
 98 cardiometabolic trait cluster while atrial fibrillation, for which T2D and CVD are risk factors³⁸, did not. Our
 99 final set of prioritized, age-associated traits included 24 genetically diverse, heritable phenotypes (**Table**
 100 **S1**). Of these, 11 traits were sufficiently heritable only in UKB, 3 were sufficiently heritable only among
 101 non-UKB meta-analyses, and 10 were well-powered in both UKB and an independent cohort.

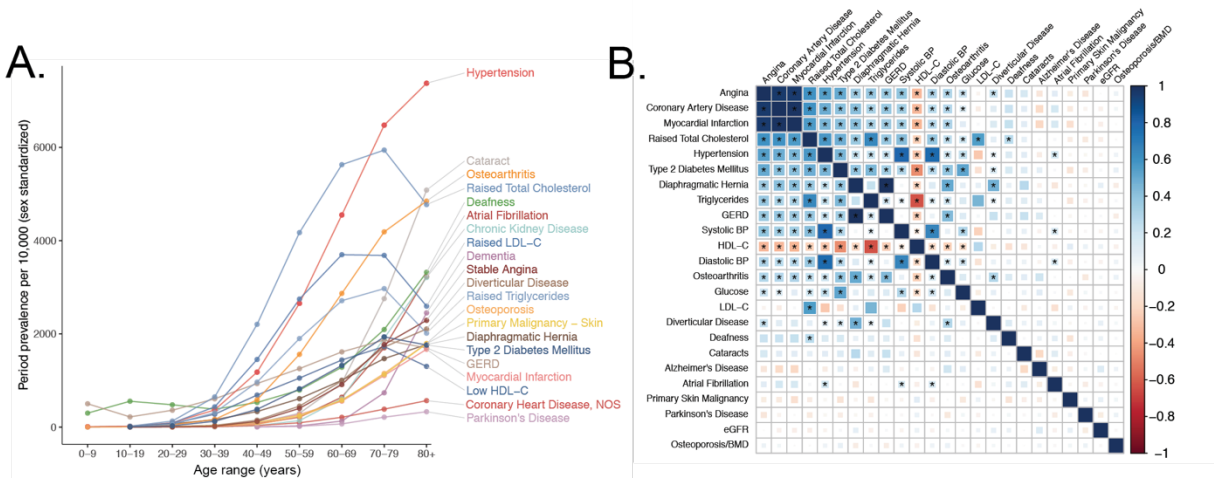


Figure 1. Selection of genetically diverse age-related diseases and traits using epidemiological data. **A.** Period prevalence of age-associated diseases systematically selected for this study (**Methods**). Epidemiological data obtained from Kuan et al. 2019. **B:** Genetic correlation between the selected age-related traits. All correlations were assessed between UK Biobank phenotypes with the exception of eGFR, Alzheimer's Disease, and Parkinson's Disease, for which the respective meta-analyses were used (**Methods**). Point estimates and standard errors reported in **Table S2**. * represent genetic correlations that are significantly different from 0 at a Bonferroni-corrected threshold for $p = 0.05 \times 24$ traits.

102

103 **No evidence for enrichment of age-related trait heritability in mitochondria-relevant loci**

104 To test if age-related trait heritability was enriched among mitochondria-relevant loci, we began by simply
 105 asking if ~1100 nucDNA genes encoding the mitochondrial proteome from the MitoCarta2.0 inventory²²
 106 were found near lead SNPs for our selected traits represented in the NHGRI-EBI GWAS Catalog
 107 (<https://www.ebi.ac.uk/gwas/>)³⁹ more frequently than expectation (**Methods, Supplementary note**). To
 108 our surprise, no traits showed a statistically significant enrichment of mitochondrial genes (**Figure S1A**);
 109 in fact, six traits showed a statistically significant depletion. Even more strikingly, MitoCarta genes tended
 110 to be nominally enriched in fewer traits than the average randomly selected sample of protein-coding
 111 genes (**Figure S1B**, empirical $p = 0.014$). This lack of enrichment was observed more broadly across
 112 virtually all traits represented in the GWAS Catalog (**Figure S1C**). We also tested several transcriptional
 113 regulators of mitochondrial biogenesis and function – *TFAM*, *GABPA*, *GABPB1*, *ESRRA*, *YY1*, *NRF1*,
 114 *PPARGC1A*, *PPARGC1B*. We found little evidence supporting a role for these genes in modifying risk for
 115 the age-related GWAS Catalog phenotypes, observing only a single trait (heel bone mineral density) for
 116 which a mitochondrial transcriptional regulator (*TFAM*) was nearest an associated genome-wide
 117 significant variant (**Supplementary note**).

118 To investigate further, we turned to U.K. Biobank (UKB). We compiled and tested three classes of
 119 “mitochondria-relevant loci” (**Figure 2A**) with which we interrogated the association between common
 120 mitochondrial variation and common disease. First, we curated literature-reported nucDNA quantitative
 121 trait loci (QTLs) associated with measures of mitochondrial function (**Table S3**): mtCN^{40,41}, mtRNA

122 abundance and modification^{42,43}, and plasma levels of OXPHOS dysfunction biomarkers including GDF15
 123 protein^{44,45}, lactate, pyruvate, and lactate/pyruvate ratio^{46–48}. Second, we considered all common variants
 124 in or near nucDNA MitoCarta genes, as well as two subsets of MitoCarta: mitochondrial Mendelian disease
 125 genes⁴⁹ and nucDNA-encoded OXPHOS genes. Third, we obtained mtDNA genotypes at up to 213 loci after
 126 quality control (**Methods**) from 360,662 individuals.

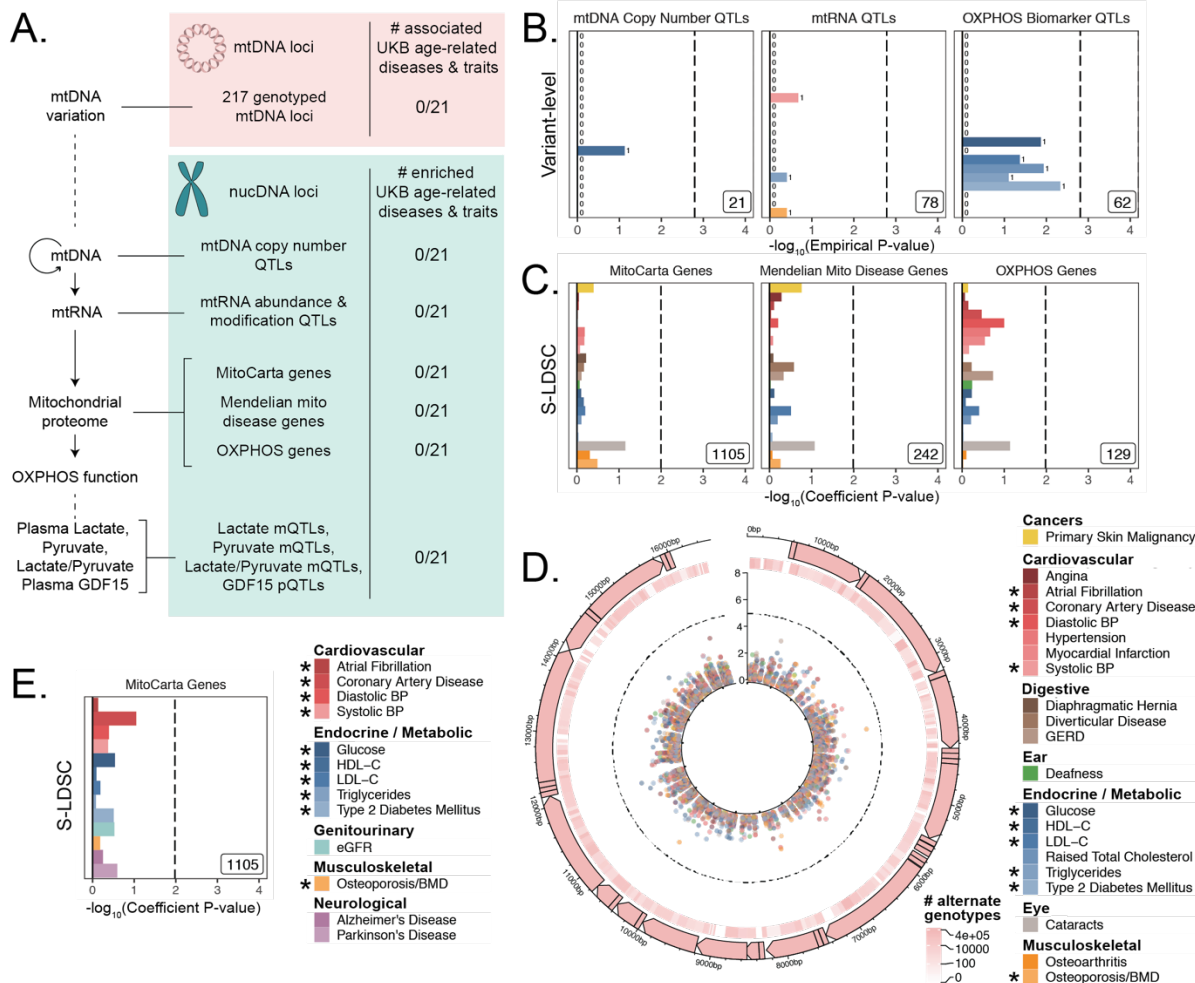


Figure 2. Assessment of the association of nucDNA and mtDNA mitochondria-relevant loci to age-related traits. **A.** Scheme outlining the aspects of mitochondrial function assessed in this study. nucDNA loci relevant to mitochondrial function are shown in teal, while mtDNA loci are shown in pink. **B.** Enrichment results for the overlap between loci associated with mtDNA copy number, mtRNA abundance/modification, and OXPHOS biomarkers and loci significantly associated with age-related disease in UKB. Inset number represents the number of tested SNPs, numbers adjacent to bars represent the absolute number of mitochondria-relevant loci overlapping the respective age-related disease. Dotted line represents Bonferroni cutoff for $p = 0.1$; BH FDR 0.1 threshold cannot be visualized as no tests pass the cutoff (**Supplementary note**). **C.** S-LDSC enrichment p-values on top of the baseline model in UKB. Inset labels represent gene-set size; dotted line represents BH FDR 0.1 threshold. **D.** Visualization of mtDNA variants and associations with age-related diseases. The outer-most track represents the genetic architecture of the circular mtDNA. The heatmap track represents the number of individuals with alternate genotype on log scale. The inner track represents mitochondrial genome-wide association p-values, with radial angle corresponding to position on the mtDNA and magnitude representing $-\log_{10}$ P-value. Dotted line represents Bonferroni cutoff for all tested trait-variant pairs. **E.** Replication of S-LDSC enrichment results in meta-analyses. Dotted line represents BH FDR 0.1 threshold. * represent traits for which sufficiently well powered cohorts from both UKB and meta-analyses were available. The trait color legend to the right of panel **D** applies to panels **B**, **C**, and **D**, representing UKB traits.

127

128 First, we tested if published QTLs for mtCN, mtRNA abundance, and OXPHOS biomarkers (**Table S3, S4**)
129 were enriched for an overlap with genome-wide significant loci for each of our age-related traits in UKB
130 (**Methods, Figure S2**). We observed no evidence of enrichment among QTLs available in the literature
131 (**Figure 2B, Supplementary note**; all $q > 0.1$).

132 Second, we used S-LDSC^{36,50} and MAGMA (<https://ctg.cncr.nl/software/magma>)⁵¹, two robust methods
133 that can be used to assess gene-based heritability enrichment accounting for LD and several confounders,
134 to test if there was any evidence of heritability enrichment among MitoCarta genes (**Methods**). We found
135 no evidence of enrichment near nucDNA MitoCarta genes for any trait tested in UKB using S-LDSC (**Figure**
136 **2C, S8A**), consistent with our results from the GWAS Catalog. We replicated this lack of enrichment using
137 MAGMA at two different window sizes (**Figure S8C, S8E**; all $q > 0.1$).

138 Given the lack of enrichment among the MitoCarta genes, we wanted to (1) verify that our selected
139 methods could detect previously reported enrichments and (2) confirm that common variation in or near
140 MitoCarta genes can lead to expression-level perturbations. We first successfully replicated previously
141 reported enrichment among tissue-specific genes for key traits using both S-LDSC (**Figure S3, S4**) and
142 MAGMA (**Figure S5, S6, Supplementary note, Methods**). We next confirmed that we had sufficient power
143 using both S-LDSC and MAGMA to detect physiologically relevant enrichment effect sizes among
144 MitoCarta genes (**Figure S7, Methods, Supplementary note**). We finally examined the landscape of cis-
145 expression QTLs (eQTLs) for these genes and found that almost all MitoCarta genes have cis-eQTLs in at
146 least one tissue and often have cis-eQTLs in more tissues than most protein-coding genes (**Figure S9,**
147 **Methods, Supplementary note**). Hence, our selected methods could detect physiologically relevant
148 heritability enrichments among our selected traits at gene-set sizes comparable to that of MitoCarta, and
149 common variants in or near MitoCarta genes exerted *cis*-control on gene expression.

150 Third, we considered mtDNA loci genotyped in UKB, obtaining calls for up to 213 common variants passing
151 quality control across 360,662 individuals (**Methods, Supplementary note**). We found no significant
152 associations on the mtDNA for any of the 21 age-related traits available in UKB using linear or logistic
153 regression (**Methods, Figure 2E, S9**).

154 As a control and to validate our approach, we also performed mtDNA-GWAS for specific traits with
155 previously reported associations. A recent analysis of ~147,437 individuals in BioBank Japan revealed four
156 distinct traits with significant mtDNA associations⁵². Of these, creatinine and aspartate aminotransferase
157 (AST) had sufficiently large sample sizes in UKB. We observed a large number of associations throughout
158 the mtDNA for both traits ($p < 1.15 * 10^{-5}$, **Figure S9E**). Thus, our mtDNA association method was able to
159 replicate robust mtDNA associations among well-powered traits.

160 Finally, we sought to replicate our negative results in an independent cohort. We turned to published
161 GWAS meta-analyses²⁶⁻³⁵ (**Table S1**) and successfully replicated the lack of enrichment for MitoCarta
162 genes across all 10 traits with an available independent cohort GWAS using S-LDSC (**Figure 2E, S8B**) and
163 MAGMA at two different window sizes (**Figure S8D, Supplementary note**; all $q > 0.1$). Importantly, while
164 we were unable to pursue analyses for PD and Alzheimer's disease in UKB due to limited case counts, we
165 tested MitoCarta genes among well-powered meta-analyses for these disorders (**Supplementary note**)
166 and observed no enrichment (**Figure 2E**; all $q > 0.1$).

167 In summary, we tested (1) QTLs for mitochondrial physiology in UKB, (2) nucDNA loci near genes that
168 encode the mitochondrial proteome in the GWAS Catalog, UKB, and GWAS meta-analyses, (3) mtDNA
169 variants in UKB, and (4) known transcriptional regulators of mitochondrial biogenesis and function in the
170 GWAS Catalog. We found no convincing evidence of heritability enrichment for common age-associated
171 diseases among these mitochondria-relevant loci (**Table S8**).

172 **Enrichment of age-related trait heritability near genes encoding nuclear transcription factors**

173 We next asked whether heritability for age-related diseases and traits clusters among loci associated with
 174 any cellular organelle. We used the COMPARTMENTS database (<https://compartments.jensenlab.org>) to
 175 define gene-sets corresponding to the proteomes of nine additional organelles⁵³ besides mitochondria
 176 (**Methods**). We used S-LDSC to produce heritability estimates for these categories in the UKB age-related
 177 disease traits, finding evidence of heritability enrichment in many traits for genes comprising the nuclear
 178 proteome (**Figure 3A, Methods**). No other tested organelles showed evidence of heritability enrichment.
 179 Variation in or near genes comprising the nuclear proteome explained over 50% of disease heritability on
 180 average despite representing only ~35% of tested SNPs (**Figure S10, Supplementary note**). We
 181 successfully replicated this pattern of heritability enrichment among organelles using MAGMA in UKB at
 182 two window sizes (**Figure S13A, S13B**), again finding only enrichment among genes related to the nucleus.

183 With over 6,000 genes comprising the nuclear proteome, we considered largely disjoint subsets of the
 184 organelle's proteome to trace the source of the enrichment signal^{54–56} (**Figure 3B, Methods,**
 185 **Supplementary note**). We found significant heritability enrichment within the set of 1,804 genes whose
 186 protein products are annotated to localize to the chromosome itself ($q < 0.1$ for 9 traits, **Figure 3C, S12**).
 187 Further partitioning revealed that much of this signal is attributable to the subset classified as
 188 transcription factors⁵⁶ (1,523 genes, $q < 0.1$ for 10 traits, **Figure 3D, S12**). We replicated these results using
 189 MAGMA in UKB at two window sizes (**Figure S13**), and also replicated enrichments among TFs in several
 190 (but not all) corresponding meta-analyses (**Figure S14**) despite reduced power (**Figure S7H**). We generated
 191 functional subdivisions of the TFs (**Methods, Supplementary note**), finding that the non-zinc finger TFs

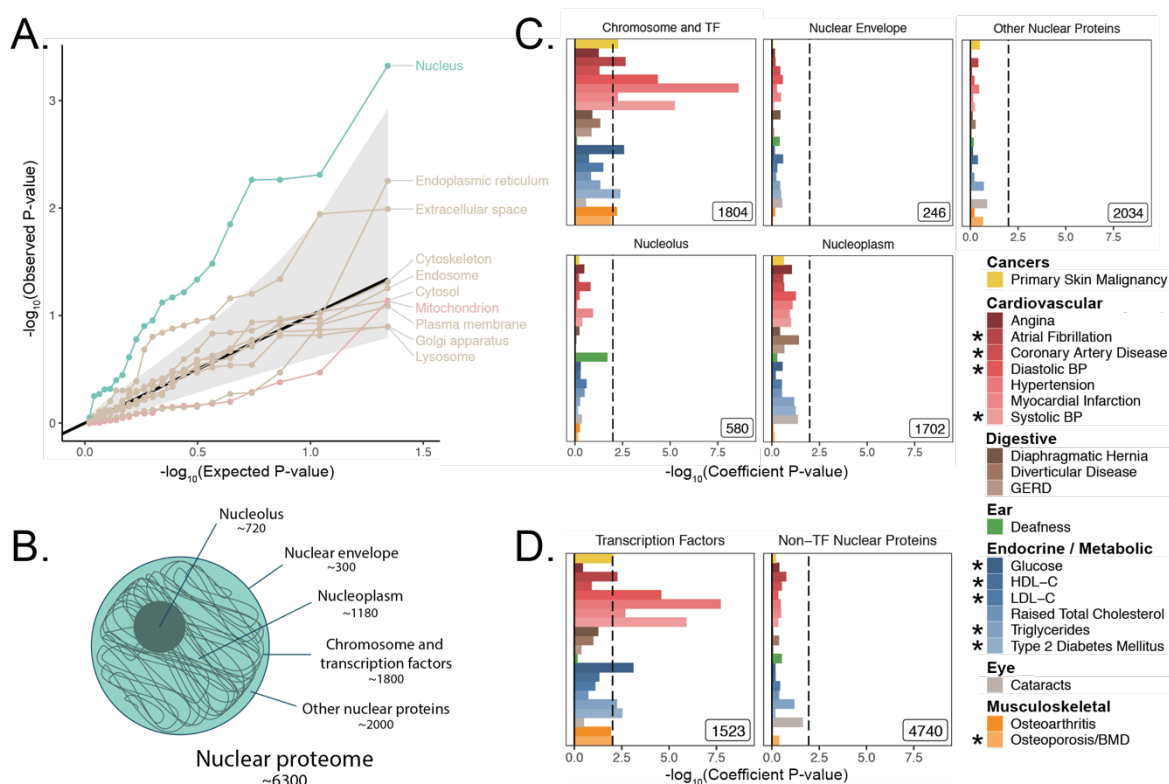


Figure 3. Heritability enrichment of organellar proteomes across age-related disease in UK Biobank. **A.** Quantile-quantile plot of heritability enrichment p-values atop the baseline model for gene-sets representing organellar proteomes, with black line representing expected null p-values following the uniform distribution and shaded ribbon representing 95% CI. **B.** Scheme of spatially distinct subsets of the nuclear proteome as a strategy to characterize observed enrichment of the nuclear proteome. Numbers represent gene-set size. **C.** S-LDSC enrichment p-values for spatial subsets of the nuclear proteome computed atop the baseline model. **D.** S-LDSC enrichment p-values for TFs and all other nucleus-localizing proteins. Inset numbers represent gene-set sizes, black lines represent cutoff at BH FDR < 10%. * represent traits for which sufficiently well powered cohorts from both UKB and meta-analyses were available.

192 showed enrichment for a highly similar set of traits to those enriched for the whole set of TFs (**Figure**
 193 **S15D, S16B, S17B, S18B**). Interestingly, the KRAB domain-containing zinc fingers (KRAB ZFs)⁵⁷, which are
 194 recently evolved (**Figure S15H**), were largely devoid of enrichment even compared to non-KRAB ZFs
 195 (**Figure S15E, S16C, S17C, S18C**). Thus, we find that variation within or near non-KRAB domain-containing
 196 transcription factor genes has an outside influence on age-associated disease heritability (**Table S8**).

197

198 **Mitochondrial genes tend to be more “haplosufficient” than genes encoding other organelles**

199 In light of observing heritability enrichment only among nuclear transcription factors, we wanted to
 200 determine if the fitness cost of pLoF variation in genes across cellular organelles mirrored our results.
 201 Mitochondria-localizing genes and TFs play a central role in numerous Mendelian diseases^{49,58–60}, so we
 202 initially hypothesized that genes belonging to either category would be under significant purifying
 203 selection (i.e., constraint). We obtained constraint metrics from gnomAD

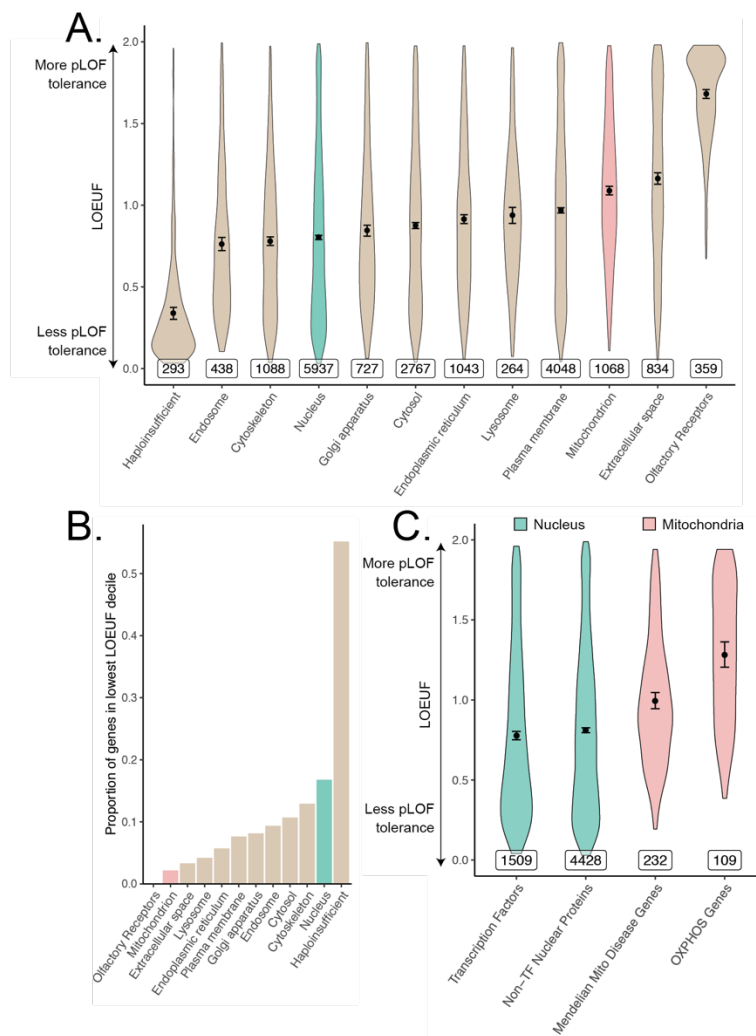


Figure 4. Differences in constraint distribution across organelles. **A.** Constraint as measured by LOEUF from gnomAD v2.1.1 for genes comprising organellar proteomes, book-ended by distributions for known haploinsufficient genes as well as olfactory receptors. Lower values indicate genes exacting a greater organismal fitness cost from a heterozygous LoF variant (greater constraint). **B.** Proportion of each gene-set found in the lowest LOEUF decile. Higher values indicate gene-sets containing more highly constrained genes. **C.** Constraint distributions for subsets of the nuclear-encoded mitochondrial proteome (red) and subsets of the nucleus (teal). Black points represent the mean with 95% CI. Inset numbers represent gene-set size.

204 (<https://gnomad.broadinstitute.org>)⁶¹ as the LoF observed/expected fraction (LOEUF). In agreement with
205 our GWAS enrichment results, we observed that the mitochondrion on average is one of the least
206 constrained organelles we tested, in stark contrast to the nucleus (**Figure 4A**). In fact, the nucleus was
207 second only to the set of “haploinsufficient” genes (defined based on curated human clinical genetic
208 data⁶¹, **Methods**) in the proportion of its genes in the most constrained decile, while the mitochondrion
209 lay on the opposite end of the spectrum (**Figure 4B**). Interestingly, even the Mendelian mitochondrial
210 disease genes had a high tolerance to pLoF variation on average in comparison to TFs (**Figure 4C, S19A**).
211 Even across different categories of TFs, we observed that highly constrained TF subsets tend to show
212 GWAS enrichment (**Figure S19B, S15E**) relative to unconstrained subsets for our tested traits. Indeed,
213 explicit inclusion of LOEUF as a covariate in the enrichment analysis model (**Methods**) reduced the
214 significance of (but did not eliminate) the enrichment seen for the TFs (**Figure S20B, S21B, S20E, S20F**).
215 Thus, while disruption in both mitochondrial genes and TFs can produce rare disease, the fitness cost of
216 heterozygous variation in mitochondrial genes appears to be far lower than that among the TFs. This
217 dichotomy reflects the contrasting enrichment results between the mitochondrial genes and the TFs and
218 supports the importance of gene regulation as it relates to evolutionary conservation.

219

220 **Discussion**

221 Pathology in cellular organelles has been widely documented in age-related diseases^{3,7,62–65}. Using a
222 human genetics approach, here we report the unexpected discovery that except for the nucleus, cellular
223 organelles tend not to be enriched in genetic associations for common, age-related diseases. We started
224 with a focus on the mitochondria as a decline in mitochondrial abundance and activity has long been
225 reported as one of the most consistent correlates of aging^{9,14,19,20} and age-associated diseases^{10–13,15–18,21}.
226 We tested mitochondria-relevant common variants on the nucDNA and mtDNA and found no convincing
227 evidence of heritability enrichment in any tested trait, cohort, or method. We systematically expanded
228 our analysis to survey 10 organelles and found that only the nucleus showed enrichment, with much of
229 this signal originating from nuclear transcription factors. Constraint analysis showed a substantial fitness
230 cost to heterozygous loss-of-function mutation in genes encoding the nuclear proteome, whereas genes
231 encoding the mitochondrial proteome were “haplosufficient.”

232 For highly polygenic and well-powered traits, any large fraction of the genome may explain a statistically
233 significant amount of disease heritability^{66,67}. Indeed, individual associations between mitochondria-
234 relevant loci and certain common diseases have been identified previously^{68,69}. As associations have also
235 been identified among loci relevant for other organelles, enrichment analyses can place these complex
236 genetic architectures in a broader biological context and prioritize pathways for follow-up. Importantly,
237 both MAGMA and S-LDSC are capable of detecting an enrichment even in a highly polygenic background.
238 Both methods have been used in the past to identify biologically plausible disease-relevant tissues^{36,50} and
239 pathway enrichments^{70,71} in traits across the spectrum of polygenicity, and we identify enrichments
240 among disease-relevant tissues using both methods in several highly polygenic traits.

241 While previous work has shown that common disease GWAS can be enriched for expression in specific
242 disease-relevant organs^{50,72}, our data suggest that this framework does not generally extend to organelles.
243 This finding contrasts with our classical nosology of inborn errors of metabolism that tend to be mapped
244 to “causal” organelles, e.g., lysosomal storage diseases, disorders of peroxisomal biogenesis, and
245 mitochondrial OXPHOS disorders. The observed enrichment for transcription factors within the nucleus
246 indicates that common variation influencing genome regulation impacts common disease risk more than
247 variation influencing individual organelles.

248 Our analysis of common inherited mitochondrial variation represents, to our knowledge, the most
249 comprehensive assessment of mitochondria-relevant nucDNA and mtDNA variation in age-related

250 diseases. We replicated mtDNA associations with creatinine and AST observed previously in BioBank
251 Japan⁵², further supporting our approach. While individual mtDNA variants have been previously
252 associated with certain traits⁷³⁻⁷⁵, these associations appear to be conflicting in the literature, perhaps
253 because of limited power and/or uncontrolled confounding biases such as population stratification^{76,77}.
254 Our negative results are surprising, but they are not inconsistent with a small number of isolated reports
255 interrogating either mitochondria-relevant nucDNA⁷⁸ or mtDNA^{52,79-81} loci in select diseases.

256 To our knowledge, we are the first to systematically document heterogeneity in average pLoF across
257 cellular organelles. That MitoCarta genes are “haplosufficient” and pLoF tolerant (**Figure 4A**) is consistent
258 with the observation that most of the ~300 inborn mitochondrial disease genes produce disease with
259 recessive inheritance⁴⁹ and healthy parents. The few mitochondrial disorders that show dominant
260 inheritance are nearly always due to dominant negativity rather than haploinsufficiency. The intolerance
261 of TFs to pLoF variation (**Figure 4A**) provide a stark contrast to the results from the mitochondria that is
262 borne out in their associated Mendelian disease syndromes: TFs are known to be haploinsufficient⁸² and
263 even regulatory variants modulating their expression can produce severe Mendelian disease⁸³. We
264 observe heritability enrichment among TFs for 10 different diseases, consistent with observed elevated
265 purifying selection against pLoF variants in these genes. Our enrichment results combined with pLoF
266 intolerance suggest that variation among TFs may produce disease-associated variants with larger effect
267 sizes than expectation, underscoring their importance as genetic “levers” for common disease heritability.

268 Why are mitochondria so robust to variation in gene dosage and hence “haplosufficient?” We propose
269 three possibilities. First, one possibility is pathway redundancy. For example, in cell culture, defective
270 OXPHOS can be supported thanks to the action of non-mitochondrial pathways such as cytosolic glycolysis
271 and nucleotide salvage as long as key environmental nutrients are provided⁸⁴. Second, mitochondrial
272 pathways tend to be highly interconnected, and it was already proposed by Wright⁸⁵ and later by Kacser
273 and Burns⁸⁶ that haplosufficiency arises as a consequence of physiology, i.e., network organization of
274 metabolic reactions. Kacser and Burns in fact explicitly mention that noncatalytic gene products fall
275 outside their framework, and we believe that our finding that nucleus-localizing and cytoskeletal genes
276 are the two most pLoF-intolerant compartments is consistent with their assessment. Third, mitochondria
277 were formerly autonomous microbes and hence may have retained vestigial layers of “intra-organelle
278 buffering” against genetic variation. Numerous feedback control mechanisms, including respiratory
279 control⁸⁷, help to ensure organelle robustness across physiological extremes^{88,89}. In fact, a recent CRISPR
280 screen showed that of the genes for which knock-out modified survival under a mitochondrial poison,
281 there is a striking over-representation of genes that themselves encode mitochondrial proteins⁹⁰.

282 Throughout this study, we have tested inherited common variant associations via an additive genetic
283 model. We acknowledge the limitations of focusing on a specific genetic model and variant frequency
284 regime, though note that common variation is the largest documented source of narrow-sense
285 heritability, which typically accounts for a majority of disease heritability^{91,92}. First, we consider only
286 common variants. While rare variants may prove to be instructive, it is notable that a previous rare variant
287 analysis in T2D⁹³ failed to show enrichment among OXPHOS genes. Second, we consider only additive
288 genetic models. A recessive model may be particularly fruitful for mitochondria-relevant loci given their
289 tolerance to pLoF variation, however these models are frequently power-limited and may not explain
290 much more phenotypic variance than additive models^{94,95}. Third, we have not considered epistasis. The
291 effects of mtDNA-nucDNA interactions⁹⁶ in common diseases have yet to be assessed. While there is
292 debate about whether biologically-relevant epistasis can be simply captured by main effects^{92,94,97,98} at
293 individual loci, it is possible that modeling mtDNA-nucDNA interactions will reveal new contributions.
294 Finally, it is crucial not to confuse our results with previously reported associations between somatic
295 mtDNA mutations and age-associated disease¹⁸⁻²⁰ – the present work is focused on germline variation.

296 We emphasize that our study does not formally address the causality of mitochondrial dysfunction in
297 common age-related disease. Rather, we have tested if common variants in mitochondrial pathways tend
298 to explain a disproportionate amount of age-related disease heritability. The observed lack of heritability
299 enrichment in mitochondrial pathways does not preclude the possibility of a therapeutic benefit in
300 targeting the mitochondrion for age-related disease. For example, mitochondrial dysfunction is
301 documented in brain or heart infarcts following blood vessel occlusion in laboratory-based models^{99,100}.
302 Though mitochondrial variants do not influence infarct risk in this laboratory model, pharmacological
303 blockade of the mitochondrial permeability transition pore can mitigate reperfusion injury and infarct
304 size¹⁰¹. Future studies will be required to determine if and how the mitochondrial dysfunction associated
305 with common age-associated diseases can be targeted for therapeutic benefit.

306 Our finding that the nucleus is the only organelle that shows enrichment for common age-associated trait
307 heritability builds on prior work implicating nuclear processes in aging. Most human progeroid syndromes
308 result from monogenic defects in nuclear components¹⁰² (e.g., *LMNA* in Hutchinson-Gilford progeria
309 syndrome, *TERC* in dyskeratosis congenita), and telomere length has long been observed as a marker of
310 aging¹⁰³. Heritability enrichment of age-related traits among gene regulators is consistent with the
311 epigenetic dysregulation¹⁰⁴ and elevated transcriptional noise^{3,105} observed in aging (e.g., *SIRT6*
312 modulation influences mouse longevity¹⁰⁶ and metabolic syndrome⁶³). An important role for gene
313 regulation in common age-related disease is in agreement with both the observation that a very large
314 fraction of common disease-associated loci corresponds to the non-coding genome and the enrichment
315 of disease heritability in histone marks and transcription factor binding sites^{36,107}. Given that a
316 deterioration in several other cellular organelles has been linked to age-related traits, a future challenge
317 lies in elucidating the connection between variation influencing transcription factors and organelle
318 dysfunction in age-related disease.

319

320 **Acknowledgements**

321 We thank D. Altshuler, S.E. Calvo, H. Finucane, E.S. Lander, M.E. MacDonald, D. Palmer, E.B. Robinson,
322 A.V. Segrè, M.E. Talkowski, R.K. Walters, C.C. Winter, and members of the Mootha and Neale labs for
323 critical feedback and discussions. This research has been conducted using the UK Biobank Resource under
324 Application Number 31063. This project was supported in part by grants (NIH R35GM122455 to V.K.M.
325 and NIH T32 AG000222 to R.G.) from the National Institutes of Health. VKM is an Investigator of the
326 Howard Hughes Medical Institute.

327

328 **Data Availability**

329 Genetic correlation point estimates and standard errors plotted in Figure 1B is available in Table S2.
330 Summary statistics from mtDNA-GWAS available in Table S6. All gene-based enrichment analysis p-values
331 and point estimates are available in Table S8. Literature-reported loci associated with biomarkers of
332 mitochondrial function after clumping and QC are available in Table S4. Period prevalence data for
333 diseases in the UK can be obtained from Kuan et al. 2019. Gene-sets can be found using COMPARTMENTS
334 (<https://compartments.jensenlab.org>), MitoCarta 2.0
335 (<https://www.broadinstitute.org/files/shared/metabolism/mitocarta/human.mitocarta2.0.html>),
336 Lambert et al. 2018 (DOI: 10.1016/j.cell.2018.01.029), Frazier et al. 2019 (DOI: 10.1074/jbc.R117.809194),
337 Finucane et al. 2018 (<https://alkesgroup.broadinstitute.org/LDSCORE/>), Kapopoulou et al. 2015 (DOI:
338 10.1111/evo.12819), and the Macarthur laboratory (https://github.com/macarthur-lab/gene_lists). Gene
339 age estimates were obtained from Litman, Stein 2019 (DOI: 10.1053/j.seminoncol.2018.11.002). GWAS
340 catalog annotations can be obtained from: <https://www.ebi.ac.uk/gwas>. UKB heritability estimates can
341 be obtained at: https://nealelab.github.io/UKBB_ldsc/. UKB summary statistics can be obtained from
342 Neale lab GWAS round 2: https://github.com/Nealelab/UK_Biobank_GWAS. Annotations for the Baseline

343 v1.1 and BaselineLD v2.2 models as well as other relevant reference data, including the 1000G EUR
344 reference panel, can be obtained from <https://alkesgroup.broadinstitute.org/LDSCORE/>. eQTL and
345 expression data in human tissues can be obtained from GTEx (<https://www.gtexportal.org>). Constraint
346 estimates can be found via gnomAD: <https://gnomad.broadinstitute.org>. See citations for publicly
347 available GWAS meta-analysis summary statistics^{26–35}.

348

349 **Code Availability**

350 Our analysis leverages publicly available tools including LDSC for heritability enrichment and genetic
351 correlation (<https://github.com/bulik/ldsc>), MAGMA v1.07b for gene-set enrichment analysis
352 (<https://ctg.cncr.nl/software/magma>), PLINK v1.07 for linkage disequilibrium clumping
353 (<https://zzz.bwh.harvard.edu/plink/>), and Hail v0.2.51 for distributed computing and mtDNA GWAS
354 (<https://hail.is>).

355

356 **Competing Interests**

357 VKM is an advisor to and receives compensation or equity from Janssen Pharmaceuticals, 5am Ventures,
358 and Raze Therapeutics. BMN is a member of the scientific advisory board at Deep Genomics and RBNC
359 Therapeutics. BMN is a consultant for Camp4 Therapeutics, Takeda Pharmaceutical and Biogen. KJK is a
360 consultant for Vor Biopharma.

361

362 **Author Contributions**

363 R.G., B.M.N., and V.K.M. conceived of the project; R.G., K.J.K., D.H. designed analyses; R.G. performed
364 analyses; B.M.N., V.K.M. supervised project; R.G. and V.K.M. wrote the manuscript with input from
365 other authors.

366 **Materials and Methods**

367 Trait selection:

368 Sex-standardized period prevalence of over 300 diseases was obtained from an extensive survey of the
369 National Health Service in the UK as reported previously²⁴. To select high prevalence late-onset diseases,
370 we ranked diseases with a median onset over 50 years of age by the sum of the period prevalence of all
371 age categories above 50. We selected the top 30 diseases using this metric and manually mapped these
372 traits to similar or equivalent phenotypes with publicly available summary statistics from UKB and/or well-
373 powered meta-analyses (e.g., Parkinson's Disease and Alzheimer's Disease for dementia) resulting in 24
374 traits with data available in UKB, meta-analyses, or both (**Table S1**).

375

376 Criteria for inclusion of summary statistics:

377 We manually mapped selected age-related diseases and traits to corresponding phenotypes in UKB. In
378 parallel, we searched the literature to identify well-powered EUR-predominant GWAS (referred to as
379 meta-analyses) that (1) used primarily non-targeted arrays, (2) had publicly available full summary
380 statistics, and (3) did not enroll individuals from UKB to serve as independent replication (**Supplementary**
381 **note**). For UKB, we obtained heritability estimates (https://github.com/Nealelab/UKBB_ldsc) previously
382 computed using stratified linkage-disequilibrium score regression (S-LDSC,
383 <https://github.com/bulik/ldsc>)³⁶ atop the BaselineLD v1.1 model using reference LD scores computed
384 from 1000G EUR. For meta-analyses, we computed heritability estimates with S-LDSC atop the updated
385 BaselineLD v2.2 model using reference LD scores computed from 1000G EUR
386 (<https://alkesgroup.broadinstitute.org/LDSCORE/>). We computed the heritability Z-score, a statistic that
387 captures sample size, polygenicity, and heritability³⁶, and included only traits with heritability Z-score > 4
388 (**Supplementary note**) for further analysis.

389

390 Genetic correlations in UKB:

391 Pairwise genetic correlations, r_g , were computed using linkage-disequilibrium score correlation³⁷ on all
392 selected age-related traits with heritability Z-score > 4. We used UKB summary statistics
393 (https://github.com/Nealelab/UK_Biobank_GWAS) for all sufficiently powered traits; summary statistics
394 from meta-analyses were used for eGFR³³, Alzheimer's Disease³⁵, and Parkinson's Disease³⁴ as these traits
395 showed heritability Z-score > 4 within meta-analyses but not in UKB (**Table S1**). P-values for genetic
396 correlation represented deviation from the null hypothesis $r_g = 0$. Traits were ordered by their
397 contribution to the first eigenvector of the absolute value of the correlation matrix, with point estimates
398 and standard errors available in **Table S2**. Bonferroni correction was applied producing a p-value cutoff of
399 $0.05/\binom{24}{2} = 1.81 * 10^{-4}$.

400

401 Assessment of mitochondria-localizing genes in the GWAS Catalog:

402 We mapped variants in the GWAS Catalog (obtained on September 5th, 2019,
403 <https://www.ebi.ac.uk/gwas/>) meeting genome-wide significance ($p < 5e-8$) to genes using provided
404 annotations, producing a set of trait-associated genes for each trait. We manually selected phenotypes
405 represented in the GWAS Catalog matching our set of age-associated traits with over annotated 30 trait-
406 associated genes. For each trait, we computed the proportion of trait associated genes that were
407 mitochondria-localizing (defined via MitoCarta2.0²²) and tested for enrichment or depletion relative to
408 overall genome background using two-sided Fisher's exact tests correcting for multiple hypothesis tests
409 with the Benjamini-Hochberg (BH) procedure at FDR q-value < 0.1.

410 We also computed the test statistic N_g^{enrich} , defined as the number of age-associated traits showing a
411 nominal (not necessarily statistically significant) enrichment for a given gene-set g , for the MitoCarta
412 genes. We then generated an empirical null distribution for N_g^{enrich} . We drew 1,000 random samples of

413 protein-coding genes, where each sample contained the same number of genes as the set of
414 mitochondria-localizing genes and computed N_g^{enrich} for each of these gene-sets (**Figure S1B**). The one-
415 sided p-value, defined as $\Pr(N_g^{enrich} \leq x)$ under the null, was subsequently obtained.

416 We expanded our enrichment/depletion analysis to all 332 traits in the GWAS Catalog with over 30 trait-
417 associated genes; for enrichment or depletion testing, we used two-sided Fisher's exact tests and
418 corrected for multiple hypothesis testing with the BH procedure at FDR q-value < 0.1.

419

420 Enrichment analysis of literature-curated mitochondria-associated phenotypes:

421 We reviewed the literature for quantitative trait loci (QTLs) for mtDNA copy number (mtCN)^{40,41}, mtRNA
422 abundance/modification^{42,43}, and biomarkers of OXPHOS dysfunction (namely lactate, pyruvate,
423 lactate/pyruvate ratio⁴⁶⁻⁴⁸, and GDF15 abundance^{44,45}) (**Supplementary note**). We subsequently used
424 PLINK v1.07 (<https://zzz.bwh.harvard.edu/plink/>)¹⁰⁸ to identify independent variants for each phenotype
425 based on the 1000G EUR reference panel (**Supplementary note**). To test for overlap with UKB age-
426 associated disease traits, we divided curated variants into three classes: mtCN-related (21 variants),
427 mtRNA-related (78 variants), and OXPHOS biomarkers (62 variants). For each of the 21 UKB age-related
428 disease traits, we computed the number of genome-wide significant ($p < 5e-8$) variants that overlapped
429 the curated variants for each class, termed $N_c^{overlap}$ where c is the class. We only considered variants
430 with INFO > 0.8 and MAF > 0.001 or expected case MAC > 25. For significance testing, we generated an
431 empirical null distribution around $N_c^{overlap}$ including only variants with INFO > 0.8. For each class, we
432 drew variants at random 2500 times matching on LD score, in-sample MAF, and distance to transcription
433 start site (where the distance metric was set to 0 if the variant was located within a gene boundary). LD
434 scores per variant were generated per-chromosome with a 1 cm window using the 1000G EUR reference
435 panel. The $N_c^{overlap}$ was then computed for each category for each set of randomly selected variants,
436 generating a category specific empirical null distribution for the statistic (**Figure S2**). The one-sided p-
437 value, defined as $\Pr(N_c^{overlap} \geq x)$ under the null, was subsequently obtained. To correct for multiple
438 hypothesis testing, we applied the BH procedure with FDR < 0.1 and also applied a Bonferroni threshold
439 of $P = \frac{0.1}{21*3} \approx 0.0016$.

440

441 Harmonization and filtering of summary statistics for LDSC and MAGMA:

442 UKB summary statistics previously formatted for use with LDSC and filtered to HapMap3 (HM3) SNPs
443 (https://github.com/Nealelab/UKBB_Idsc) were used for analysis with S-LDSC. For analysis with MAGMA
444 v1.07b⁵¹, we included variants from the full Neale Lab UKB Round 2 GWAS summary statistics
445 (https://github.com/Nealelab/UK_Biobank_GWAS) with INFO > 0.8 and MAF > 0.01, and excluded any
446 variants flagged as low confidence (a heuristic defined by MAF < 0.001 or expected case MAC < 25).

447 Summary statistics obtained from publicly available GWAS meta-analyses²⁶⁻³⁵ were reported in varied
448 formats. We manually verified the genome build upon which each meta-analysis reported results and
449 ensured that all sets of summary statistics contained columns listing P-value, variant rsID, genome-build
450 specific coordinates, and if available, variant-specific sample size (**Table S1**). If variant coordinates or rsID
451 were not provided, the relevant columns were obtained from dbSNP database version 130 (for hg18) or
452 146 (for hg19). We used the summary statistic munging script provided with S-LDSC
453 (<https://github.com/bulik/ldsc>) to generate summary statistics compatible with S-LDSC, restricting to
454 HM3 SNPs as these tend to be best behaved for analysis with LDSC. For use of meta-analyses with
455 MAGMA⁵¹, we restricted analysis to variants with INFO > 0.8 and MAF > 0.01 if such information was
456 provided.

457

458 Multiple testing correction for gene-set enrichment analysis:

459 To account for the multiple hypothesis tests performed throughout this study, we obtained p-value
460 thresholds via the BH procedure at FDR < 0.1 for all gene-sets assessed for a given method and cohort
461 type (where the two cohort types were UKB and meta-analysis).

462

463 Gene-set based enrichment analysis:

464 We extensively use S-LDSC and MAGMA to perform gene-set enrichment analyses among GWAS summary
465 statistics. To test enrichment with S-LDSC, SNPs were mapped to each gene with a 100kb symmetric
466 window as recommended⁵⁰ and LD scores were computed using the 1000G EUR reference panel
467 (<https://alkesgroup.broadinstitute.org/LDSCORE/>) and subsequently restricted to the HM3 SNPs. We
468 used S-LDSC to test for heritability enrichment controlling for 53 annotations including coding regions,
469 enhancer regions, 5' and 3' UTRs, and others as previously described³⁶ (baseline v1.1, referred to as
470 baseline model hereafter). We also used MAGMA with both 5kb up, 1.5kb down and 100kb symmetric
471 windows to test for enrichment. MAGMA gene-level analysis was performed with the 1000G EUR LD
472 reference panel to account for LD structure, and gene-set analysis was performed including covariates for
473 gene length, variant density, inverse minor allele count (MAC), as well as log-transformed versions of
474 these covariates. Statistical tests for both S-LDSC and MAGMA were one-sided, considering enrichment
475 only. For both methods, we included the relevant superset of genes as a control to ensure that our analysis
476 was competitive (**Supplementary note**). We refer to this approach as the 'usual approach'. All enrichment
477 effect size estimates and p-values are available in **Table S8**.

478

479 Enrichment analysis of genes comprising the mitochondrial proteome:

480 We obtained the set of nuclear-encoded mitochondria-localizing genes using MitoCarta2.0²² and used the
481 literature to obtain the subset of MitoCarta genes involved in inherited mitochondrial disease⁴⁹ as well as
482 those producing components of oxidative phosphorylation (OXPHOS) complexes. We used both S-LDSC
483 and MAGMA to test for enrichment in the usual way (**Methods**) controlling for the set of protein-coding
484 genes to ensure a competitive analysis (**Supplementary note**). We also tested mitochondria-localizing
485 genes for enrichment in meta-analyses using S-LDSC and MAGMA with the same parameters as for UKB
486 traits (**Supplementary note**).

487

488 Tissue-expressed gene-set enrichment analysis:

489 To obtain the set of genes most expressed in a given tissue versus others, we obtained t-statistics
490 computed from GTEx v6 gene-level transcript-per-million (TPM) data corrected for age and sex as
491 published previously⁵⁰. For each tissue, we selected the top 2485 genes (10%) with the highest t-statistics
492 for tissue-specific expression, producing tissue-expressed gene-sets. We selected nine tissues based on
493 expectation of enrichment for our tested traits in UKB (e.g., liver for LDL levels, esophageal mucosa for
494 GERD). We used both S-LDSC and MAGMA to test for enrichment in the usual way (**Methods**) controlling
495 for the set of tissue-expressed genes to ensure a competitive analysis (**Supplementary note**). Tissue-
496 expressed gene-set analyses were performed on meta-analyses with S-LDSC and MAGMA on the same
497 tissues using the same parameters as used in UKB.

498

499 Power analysis:

500 To test for the effects of gene-set size on power, we selected ten positive control tissue-trait pairs based
501 on (1) the presence of tissue enrichment in UKB with S-LDSC and MAGMA and (2) if the observed
502 enrichment was biologically plausible. The pairs tested were liver-HDL, liver-LDL, liver-TG, liver-
503 cholesterol, pancreas-glucose, pancreas-type 2 diabetes, atrial appendage-atrial fibrillation, sigmoid
504 colon-diverticular disease, coronary artery-myocardial infarction, and visceral adipose-HDL. We then, in
505 brief, used an empirical sampling-based approach, generating random subsamples of a selected set of
506 tissue-expressed gene-sets at four different gene-set sizes (1523, 1105, 800, and 350 genes), defining

507 power as the proportion of trials showing a significant enrichment (**Supplementary note**). We used the
508 same sub-sampled gene-sets for enrichment analysis using both S-LDSC and MAGMA in the usual way
509 (**Methods**) controlling for the set of tissue-expressed genes to ensure a competitive analysis
510 (**Supplementary note**). We used the same gene-sets among the subset of the positive control traits that
511 showed enrichment in the corresponding meta-analysis to verify power for the meta-analyses
512 (**Supplementary note**).

513

514 Cross-tissue eQTL analysis

515 We obtained the set of eGenes from GTEx v8 across 49 tissues (<https://www.gtexportal.org>), filtering to
516 only include cis-eQTLs with q-value < 0.05. To determine how the landscape of cis-eQTLs for MitoCarta
517 genes compared to other protein-coding genes, we regressed the number of tissues with a detected cis-
518 eQTL for a given gene x , N_x^{eQTL} , onto an indicator for membership in a given organellar proteome
519 ($I_x^{organelle}$), controlling for gene length, log gene length, breadth of expression (τ_x), and the number of
520 tissues with detected expression > 5 TPM ($N_x^{express}$, **Supplementary note**). To quantify breadth of
521 expression, we obtained median-per-tissue GTEx v8 TPM expression values and computed τ^{109} after
522 removing lowly-expressed genes with maximal cross-tissue TPM < 1, defined as:

523

$$524 \quad \tau_x = \frac{\sum_{i=1}^n (1 - \hat{x}_i)}{n - 1} \text{ where } \hat{x}_i = \frac{x_i}{\max_{1 \leq i \leq n} x_i}$$

525

526 where x_i is the expression of gene x in tissue i with n tissues. τ ranges from 0 to 1, with lower τ indicating
527 broadly expressed gene and higher τ indicating more tissue specific expression patterns. Because GTEx
528 sampled multiple tissue subtypes (e.g., brain sub-regions) that show correlated expression profiles¹¹⁰
529 which bias τ_x , N_x^{eQTL} , and $N_x^{express}$ upward, for each broader tissue class (brain, heart, artery, esophagus,
530 skin, cervix, colon, adipose) we selected a single representative tissue when computing these quantities
531 (**Figure S14B, Supplementary note**). We used LD scores computed from the 1000G EUR reference panel.
532 The model, fit via OLS for each tested organelle, was:

533

$$534 \quad N_x^{eQTL} \sim I_x^{organelle} + N_x^{express} + \tau_x + \log(\text{gene length}) + \text{gene length}$$

535

536 mtDNA-wide association study:

537 We obtained mtDNA genotype data on 265 variants as obtained on the UK Biobank Axiom array and the
538 UK BiLEVE array from the full UKB release²⁵. To perform variant QC, we used evoker-lite¹¹¹ to generate
539 fluorescence cluster plots per-variant and per-batch and manually inspected the results, removing 19
540 variants due to cluster plot abnormalities (**Table S5, Supplementary note**). We additionally removed any
541 variants with heterozygous calls, within-array-type call rate < 0.95, and with less than 20 individuals with
542 an alternate genotype. For case-control traits, we removed any phenotype-variant pair with an expected
543 case count of alternate genotype individuals of less than 20, resulting in a maximum of 213 variants tested
544 per trait (**Supplementary note**). To perform sample QC, we restricted samples to the same samples from
545 which UKB summary statistics were generated (https://github.com/Nealelab/UK_Biobank_GWAS),
546 namely unrelated individuals 7 standard deviations away from the first 6 European sample selection PCs
547 with self-reported white-British, Irish, or White ethnicity and no evidence of sex chromosome aneuploidy.
548 We additionally removed any samples with within-array-type mitochondrial variant call rate < 0.95,
549 resulting in 360,662 unrelated samples of EUR ancestry. We generated the LD matrix for mitochondrial
550 DNA variants using Hail v0.2.51 (<https://hail.is>) pairwise for all 213 variants tested across all post-QC
551 samples.

552 We ran mtDNA-GWAS for all 21 UKB age-related phenotypes as well as creatinine and AST using Hail
553 v0.2.51 via linear regression controlling for the first 20 PCs of the nuclear genotype matrix, sex, age, age²,
554 sex*age, and sex*age² as performed for the UKB GWAS
555 (https://github.com/Nealelab/UK_Biobank_GWAS). We also used Hail to run Firth logistic regression with
556 the same covariates for case/control traits (**Table S1**). As we observed that some mitochondrial DNA
557 variants were specific to array type, we also ran linear regression including array type as a covariate; we
558 did not perform logistic regression with array type as a covariate due to convergence issues secondary to
559 complete separation of variants assessed only on only array type. We defined mtDNA-wide significance
560 using a Bonferroni correction by $p = \frac{0.05}{4337} \approx 1.15e - 5$.

561

562 *Enrichment analysis of components of organellar proteomes:*

563 COMPARTMENTS (<https://compartments.jensenlab.org>)⁵³ is a resource integrating several lines of
564 evidence for protein localization predictions including annotations, text-mining, sequence predictions,
565 and experimental data from the Human Protein Atlas. We used this resource to obtain the degree of
566 evidence (a number ranging from 0 to 5) linking each gene to localization to one of 12 organelles: nucleus,
567 cytosol, cytoskeleton, peroxisome, lysosome, endoplasmic reticulum, Golgi apparatus, plasma
568 membrane, endosome, extracellular space, mitochondrion, and proteasome. To avoid noisy localization
569 assignments due to weak text mining and prediction evidence, we only considered localization
570 assignments with a score > 2 as described previously⁵³. We subsequently assigned compartment(s) to each
571 gene by selecting the compartment(s) with the maximal score within each gene. We only included
572 compartments containing over 240 genes due to limited power at these smaller gene-set sizes and used
573 MitoCarta2.0²² to obtain a higher confidence set of genes localizing to the mitochondrion, resulting in
574 gene-sets representing the proteomes of 10 organelles. S-LDSC and MAGMA were used to test for
575 enrichment across the UKB age-related traits for these gene-sets in the usual way, controlling for the set
576 of protein-coding genes. S-LDSC was also used to obtain estimates of the percentage of heritability
577 explained by each organelle gene-set.

578

579 *Enrichment analysis of spatial components of the nucleus:*

580 To produce interpretable sub-divisions of the nucleus, we used Gene Ontology (GO)^{54,55} to identify terms
581 listed as children of the nucleus cellular component (GO:0005634). We used Ensembl version 99¹¹² to
582 obtain a first pass set of genes annotated to each sub-compartment of the nucleus (or its children). After
583 manual review of sub-compartments with > 90 genes, we selected nucleoplasm (GO:0005654), nuclear
584 chromosome (GO:0000228), nucleolus (GO:0005730), nuclear envelope (GO:0005635), splicosomal
585 complex (GO:0005681), nuclear DNA-directed RNA polymerase complex (GO:0055029), and nuclear pore
586 (GO:0005643). We excluded terms listed as 'part' due to poor interpretability and manually excluded
587 similar terms (e.g., nuclear lumen vs nucleoplasm). To generate a high confidence set of genes localizing
588 to each of these selected sub-compartments, we then turned to the COMPARTMENTS resource which
589 assigns localization confidence scores for each protein to GO cellular component terms. We assigned
590 members of the nuclear proteome to these selected nuclear sub-compartments using same the approach
591 outlined for the organelle analysis (**Methods**). After filtering our selected sub-compartments to those
592 containing > 240 genes, we obtained four categories: nucleoplasm, nuclear chromosome, nucleolus, and
593 nuclear envelope. The nuclear chromosome annotation was largely overlapping with a manually curated
594 high-quality list of transcription factors⁵⁶ however was not exhaustive; as such, we merged these lists to
595 generate the chromosome and TF category. To improve interpretability, we removed genes from
596 nucleoplasm that were also assigned to another nuclear sub-compartment, constructed a list of other
597 nucleus-localizing proteins not captured in these four sub-compartments, and included only genes
598 annotated as localizing to the nucleus (**Methods**). S-LDSC and MAGMA were used to test for enrichment

599 across the UKB age-related traits for these gene-sets in the usual way while controlling for the set of
600 protein-coding genes (**Methods**).

601

602 *Enrichment analysis of functionally distinct TF subsets:*

603 We used a published curated high-quality list of TFs⁵⁶ to partition the Chromosome and TF category into
604 transcription factors and other chromosomal proteins. To determine which TFs are broadly expressed
605 versus tissue specific, we computed τ per TF across all selected tissues after removing lowly-expressed
606 genes with maximal cross-tissue TPM < 1 (**Methods, Supplementary note**). The threshold for tissue-
607 specific genes was set at $\tau \geq 0.76$ based on the location of the central nadir of the resultant bimodal
608 distribution (**Figure S14A**). To identify terciles of TFs by age, we obtained relative gene age assignments
609 for each gene previously generated by obtaining the modal earliest ortholog level across several databases
610 mapped to 19 ordered phylostrata¹¹³. DNA binding domain (DBD) annotations for the TFs were obtained
611 from previous manual curation efforts⁵⁶. S-LDSC and MAGMA were used to test for enrichment across the
612 UKB age-related traits for these gene-sets in the usual way while controlling for the set of protein-coding
613 genes (**Methods**). We also tested TFs for enrichment in meta-analyses using S-LDSC and MAGMA with the
614 same parameters as for UKB traits (**Supplementary note**).

615

616 *Analysis of constraint across organelles and sub-organelle gene-sets:*

617 We obtained gene-level gnomAD v2.1.1 constraint tables (<https://gnomad.broadinstitute.org>),
618 haploinsufficient genes, and olfactory receptors⁶¹ (https://github.com/macarthur-lab/gene_lists).
619 Constraint values as loss-of-function observed/expected fraction (LOEUF) were mapped to genes within
620 organelle, sub-mitochondrial, sub-nuclear, and TF binding domain gene-sets.

621

622 *Enrichment analysis across age-related disease holding constraint as a covariate:*

623 To test for enrichment with constraint as a covariate, we used MAGMA with UKB age-related traits. We
624 mapped variants to genes and performed the gene-level analysis as done previously for the mitochondria-
625 localizing gene and organelle analysis. We included LOEUF and log LOEUF as covariates for the gene-set
626 analysis in addition to the default covariates (gene length, SNP density, inverse MAC, as well as the
627 respective log-transformed versions) via the `-condition-residualize` flag.

- 628 1. Wang K, Gaitsch H, Poon H, Cox NJ, Rzhetsky A. Classification of common human diseases derived
629 from shared genetic and environmental determinants. *Nat Genet.* 2017;49(9):1319-1325.
630 doi:10.1038/ng.3931
- 631 2. Claussnitzer M, Cho JH, Collins R, et al. A brief history of human disease genetics. *Nature.*
632 2020;577(7789):179-189. doi:10.1038/s41586-019-1879-7
- 633 3. López-Otín C, Blasco MA, Partridge L, Serrano M, Kroemer G. The hallmarks of aging. *Cell.*
634 2013;153(6):1194. doi:10.1016/j.cell.2013.05.039
- 635 4. Mizushima N, Levine B, Cuervo AM, Klionsky DJ. Autophagy fights disease through cellular self-
636 digestion. *Nature.* 2008;451(7182):1069-1075. doi:10.1038/nature06639
- 637 5. Hara T, Nakamura K, Matsui M, et al. Suppression of basal autophagy in neural cells causes
638 neurodegenerative disease in mice. *Nature.* 2006;441(7095):885-889. doi:10.1038/nature04724
- 639 6. Komatsu M, Waguri S, Chiba T, et al. Loss of autophagy in the central nervous system causes
640 neurodegeneration in mice. *Nature.* 2006;441(7095):880-884. doi:10.1038/nature04723
- 641 7. Özcan U, Cao Q, Yilmaz E, et al. Endoplasmic Reticulum Stress Links Obesity, Insulin Action, and
642 Type 2 Diabetes. *Science (80-).* 2004;306(5695):457 LP - 461.
643 <http://science.sciencemag.org/content/306/5695/457.abstract>.
- 644 8. D'Angelo MA, Raices M, Panowski SH, Hetzer MW. Age-Dependent Deterioration of Nuclear Pore
645 Complexes Causes a Loss of Nuclear Integrity in Postmitotic Cells. *Cell.* 2009;136(2):284-295.
646 doi:10.1016/j.cell.2008.11.037
- 647 9. Fleischman A, Makimura H, Stanley TL, et al. Skeletal muscle phosphocreatine recovery after
648 submaximal exercise in children and young and middle-aged adults. *J Clin Endocrinol Metab.*
649 2010;95(9):69-74. doi:10.1210/jc.2010-0527
- 650 10. Petersen KF, Dufour S, Befroy D, Garcia R, Shulman GI. Impaired Mitochondrial Activity in the
651 Insulin-Resistant Offspring of Patients with Type 2 Diabetes. *N Engl J Med.* 2004;350(7):664-671.
652 doi:10.1056/nejmoa031314
- 653 11. Mootha VK, Lindgren CM, Eriksson KF, et al. PGC-1 α -responsive genes involved in oxidative
654 phosphorylation are coordinately downregulated in human diabetes. *Nat Genet.* 2003;34(3):267-
655 273. doi:10.1038/ng1180
- 656 12. Fannin SW, Lesnefsky EJ, Slabe TJ, Hassan MO, Hoppel CL. Aging selectively decreases oxidative
657 capacity in rat heart interfibrillar mitochondria. *Arch Biochem Biophys.* 1999;372(2):399-407.
658 doi:10.1006/abbi.1999.1508
- 659 13. Schapira AH V, Cooper JM, Dexter D, Clark JB, Jenner P, Marsden CD. Mitochondrial Complex I
660 Deficiency in Parkinson's Disease. *J Neurochem.* 1990;54(3):823-827. doi:10.1111/j.1471-
661 4159.1990.tb02325.x
- 662 14. Trounce I, Byrne E, Marzuki S. Decline in Skeletal Muscle Mitochondrial Respiratory Chain
663 Function: Possible Factor in Ageing. *Lancet.* 1989;333(8639):637-639. doi:10.1016/S0140-
664 6736(89)92143-0
- 665 15. Kelley DE, He J, Menshikova E V., Ritov VB. Dysfunction of mitochondria in human skeletal muscle
666 in type 2 diabetes. *Diabetes.* 2002;51(10):2944-2950. doi:10.2337/diabetes.51.10.2944
- 667 16. Patti ME, Butte AJ, Crunkhorn S, et al. Coordinated reduction of genes of oxidative metabolism in
668 humans with insulin resistance and diabetes: Potential role of PGC1 and NRF1. *Proc Natl Acad Sci*
669 *U S A.* 2003;100(14):8466-8471. doi:10.1073/pnas.1032913100
- 670 17. Stump CS, Short KR, Bigelow ML, Schimke JM, Nair KS. Effect of insulin on human skeletal muscle
671 mitochondrial ATP production, protein synthesis, and mRNA transcripts. *Proc Natl Acad Sci U S A.*
672 2003;100(13):7996-8001. doi:10.1073/pnas.1332551100
- 673 18. Bender A, Krishnan KJ, Morris CM, et al. High levels of mitochondrial DNA deletions in substantia
674 nigra neurons in aging and Parkinson disease. *Nat Genet.* 2006;38(5):515-517.
675 doi:10.1038/ng1769

- 676 19. Taylor RW, Barron MJ, Borthwick GM, et al. Mitochondrial DNA mutations in human colonic crypt
677 stem cells Find the latest version : Mitochondrial DNA mutations in human colonic crypt stem
678 cells. *J Clin Invest*. 2003;112(9):1351-1360. doi:10.1172/JCI200319435. Introduction
679 20. Wanagat J, Cao Z, Pathare P, Aiken JM. Mitochondrial DNA deletion mutations colocalize with
680 segmental electron transport system abnormalities, muscle fiber atrophy, fiber splitting, and
681 oxidative damage in sarcopenia. *FASEB J*. 2001;15(2):322-332. doi:10.1096/fj.00-0320com
682 21. Ashar FN, Zhang Y, Longchamps RJ, et al. Association of mitochondrial DNA copy number with
683 cardiovascular disease. *JAMA Cardiol*. 2017;2(11):1247-1255. doi:10.1001/jamacardio.2017.3683
684 22. Calvo SE, Clauser KR, Mootha VK. MitoCarta2.0: An updated inventory of mammalian
685 mitochondrial proteins. *Nucleic Acids Res*. 2016;44(D1):D1251-D1257. doi:10.1093/nar/gkv1003
686 23. Schon EA, Dimauro S, Hirano M. Human mitochondrial DNA: Roles of inherited and somatic
687 mutations. *Nat Rev Genet*. 2012;13(12):878-890. doi:10.1038/nrg3275
688 24. Kuan V, Denaxas S, Gonzalez-Izquierdo A, et al. A chronological map of 308 physical and mental
689 health conditions from 4 million individuals in the English National Health Service. *Lancet Digit
690 Heal*. 2019;1(2):e63-e77. doi:10.1016/s2589-7500(19)30012-3
691 25. Sudlow C, Gallacher J, Allen N, et al. UK Biobank: An Open Access Resource for Identifying the
692 Causes of a Wide Range of Complex Diseases of Middle and Old Age. *PLoS Med*. 2015;12(3):1-10.
693 doi:10.1371/journal.pmed.1001779
694 26. Teslovich TM, Musunuru K, Smith A V, et al. Biological, clinical and population relevance of 95 loci
695 for blood lipids. *Nature*. 2010;466(7307):707-713. <http://dx.doi.org/10.1038/nature09270>.
696 27. Ehret GB, Munroe PB, Rice KM, et al. Genetic variants in novel pathways influence blood pressure
697 and cardiovascular disease risk. *Nature*. 2011;478(7367):103-109. doi:10.1038/nature10405
698 28. Manning AK, Hivert M-F, Scott RA, et al. A genome-wide approach accounting for body mass
699 index identifies genetic variants influencing fasting glycemic traits and insulin resistance. *Nat
700 Genet*. 2012;44(6):659-669. <http://dx.doi.org/10.1038/ng.2274>.
701 29. Morris AP, Voight BF, Teslovich TM, et al. Large-scale association analysis provides insights into
702 the genetic architecture and pathophysiology of type 2 diabetes. *Nat Genet*. 2012;44(9):981-990.
703 doi:10.1038/ng.2383
704 30. Schunkert H, König IR, Kathiresan S, et al. Large-scale association analysis identifies 13 new
705 susceptibility loci for coronary artery disease. *Nat Genet*. 2011;43(4):333-340.
706 doi:10.1038/ng.784
707 31. Estrada K, Styrkarsdottir U, Evangelou E, et al. Genome-wide meta-analysis identifies 56 bone
708 mineral density loci and reveals 14 loci associated with risk of fracture. *Nat Genet*.
709 2012;44(5):491-501. doi:10.1038/ng.2249
710 32. Christophersen IE, Rienstra M, Roselli C, et al. Large-scale analyses of common and rare variants
711 identify 12 new loci associated with atrial fibrillation. *Nat Genet*. 2017;49(6):946-952.
712 doi:10.1038/ng.3843
713 33. Pattaro C, Teumer A, Gorski M, et al. Genetic associations at 53 loci highlight cell types and
714 biological pathways relevant for kidney function. *Nat Commun*. 2016;7:1-19.
715 doi:10.1038/ncomms10023
716 34. Nalls MA, Blauwendraat C, Vallerga CL, et al. Identification of novel risk loci, causal insights, and
717 heritable risk for Parkinson's disease: a meta-analysis of genome-wide association studies. *Lancet
718 Neurol*. 2019;18(12):1091-1102. doi:10.1016/S1474-4422(19)30320-5
719 35. Lambert JC, Ibrahim-Verbaas CA, Harold D, et al. Meta-analysis of 74,046 individuals identifies 11
720 new susceptibility loci for Alzheimer's disease. *Nat Genet*. 2013;45(12):1452-1458.
721 doi:10.1038/ng.2802
722 36. Finucane HK, Bulik-Sullivan B, Gusev A, et al. Partitioning heritability by functional annotation
723 using genome-wide association summary statistics. *Nat Genet*. 2015;47(11):1228-1235.

- 724 doi:10.1038/ng.3404
- 725 37. Bulik-Sullivan B, Finucane HK, Anttila V, et al. An atlas of genetic correlations across human
726 diseases and traits. *Nat Genet.* 2015;47(11):1236-1241. doi:10.1038/ng.3406
- 727 38. Wasmer K, Eckardt L, Breithardt G. Predisposing factors for atrial fibrillation in the elderly. *J*
728 *Geriatr Cardiol.* 2017;14(3):179-184. doi:10.11909/j.issn.1671-5411.2017.03.010
- 729 39. MacArthur J, Bowler E, Cerezo M, et al. The new NHGRI-EBI Catalog of published genome-wide
730 association studies (GWAS Catalog). *Nucleic Acids Res.* 2016;45(November 2016):gkw1133.
731 doi:10.1093/nar/gkw1133
- 732 40. Cai N, Li Y, Chang S, et al. Genetic Control over mtDNA and Its Relationship to Major Depressive
733 Disorder. *Curr Biol.* 2015;25(24):3170-3177. doi:10.1016/j.cub.2015.10.065
- 734 41. Guyatt AL, Brennan RR, Burrows K, et al. A genome-wide association study of mitochondrial DNA
735 copy number in two population-based cohorts. *Hum Genomics.* 2019;13(1):6.
736 doi:10.1186/s40246-018-0190-2
- 737 42. Ali AT, Boehme L, Carbajosa G, Seitan VC, Small KS, Hodgkinson A. Nuclear genetic regulation of
738 the human mitochondrial transcriptome. *Elife.* 2019;8:1-23. doi:10.7554/eLife.41927
- 739 43. Ali AT, Idaghdour Y, Hodgkinson A. Analysis of mitochondrial m1A/G RNA modification reveals
740 links to nuclear genetic variants and associated disease processes. *Commun Biol.* 2020;3(1):1-11.
741 doi:10.1038/s42003-020-0879-3
- 742 44. Folkersen L, Fauman E, Sabater-Lleal M, et al. Mapping of 79 loci for 83 plasma protein
743 biomarkers in cardiovascular disease. *PLoS Genet.* 2017;13(4):1-21.
744 doi:10.1371/journal.pgen.1006706
- 745 45. Jiang J, Thalamuthu A, Ho JE, et al. A meta-analysis of genome-wide association studies of growth
746 differentiation factor-15 concentration in blood. *Front Genet.* 2018;9(MAR):1-13.
747 doi:10.3389/fgene.2018.00097
- 748 46. Shin SY, Fauman EB, Petersen AK, et al. An atlas of genetic influences on human blood
749 metabolites. *Nat Genet.* 2014;46(6):543-550. doi:10.1038/ng.2982
- 750 47. Suhre K, Shin SY, Petersen AK, et al. Human metabolic individuality in biomedical and
751 pharmaceutical research. *Nature.* 2011;477(7362):54-62. doi:10.1038/nature10354
- 752 48. Raffler J, Friedrich N, Arnold M, et al. Genome-Wide Association Study with Targeted and Non-
753 targeted NMR Metabolomics Identifies 15 Novel Loci of Urinary Human Metabolic Individuality.
754 *PLoS Genet.* 2015;11(9):1-28. doi:10.1371/journal.pgen.1005487
- 755 49. Frazier AE, Thorburn DR, Compton AG. Mitochondrial energy generation disorders: Genes,
756 mechanisms, and clues to pathology. *J Biol Chem.* 2019;294(14):5386-5395.
757 doi:10.1074/jbc.R117.809194
- 758 50. Finucane HK, Reshef YA, Anttila V, et al. Heritability enrichment of specifically expressed genes
759 identifies disease-relevant tissues and cell types. *Nat Genet.* 2018;50(4):621-629.
760 doi:10.1038/s41588-018-0081-4
- 761 51. de Leeuw CA, Mooij JM, Heskes T, Posthuma D. MAGMA: Generalized Gene-Set Analysis of GWAS
762 Data. *PLoS Comput Biol.* 2015;11(4):1-19. doi:10.1371/journal.pcbi.1004219
- 763 52. Yamamoto K, Sakaue S, Matsuda K, et al. Genetic and phenotypic landscape of the mitochondrial
764 genome in the Japanese population. *Commun Biol.* 2020;3(1):104. doi:10.1038/s42003-020-0812-
765 9
- 766 53. Binder JX, Pletscher-Frankild S, Tsaou K, et al. COMPARTMENTS: Unification and visualization of
767 protein subcellular localization evidence. *Database.* 2014;2014:1-9.
768 doi:10.1093/database/bau012
- 769 54. Carbon S, Douglass E, Dunn N, et al. The Gene Ontology Resource: 20 years and still GOing
770 strong. *Nucleic Acids Res.* 2019;47(D1):D330-D338. doi:10.1093/nar/gky1055
- 771 55. Ashburner M, Ball CA, Blake JA, et al. Gene Ontology: Tool for The Unification of Biology. *Nat*

- 772 *Genet.* 2000;25(1):25-29. doi:10.1038/75556
- 773 56. Lambert SA, Jolma A, Campitelli LF, et al. The Human Transcription Factors. *Cell.* 2018;172(4):650-
774 665. doi:10.1016/j.cell.2018.01.029
- 775 57. Kapopoulou A, Mathew L, Wong A, Trono D, Jensen JD. The evolution of gene expression and
776 binding specificity of the largest transcription factor family in primates. *Evolution (N Y).*
777 2016;70(1):167-180. doi:10.1111/evo.12819
- 778 58. Jimenez-Sanchez G, Childs B, Valle D. Human Disease Genes. *Nature.* 2001;409:853-855.
- 779 59. Worman HJ, Courvalin JC. The nuclear lamina and inherited disease. *Trends Cell Biol.*
780 2002;12(12):591-598. doi:10.1016/S0962-8924(02)02401-7
- 781 60. Cleaver JE. It was a very good year for DNA repair. *Cell.* 1994;76(1):1-4. doi:10.1016/0092-
782 8674(94)90165-1
- 783 61. Karczewski KJ, Francioli LC, Tiao G, et al. The mutational constraint spectrum quantified from
784 variation in 141,456 humans. *Nature.* 2020;581(7809):434-443. doi:10.1038/s41586-020-2308-7
- 785 62. Colacurcio DJ, Nixon RA. Disorders of lysosomal acidification—The emerging role of v-ATPase in
786 aging and neurodegenerative disease. *Ageing Res Rev.* 2016;32:75-88.
787 doi:10.1016/j.arr.2016.05.004
- 788 63. Kanfi Y, Peshti V, Gil R, et al. SIRT6 protects against pathological damage caused by diet-induced
789 obesity. *Aging Cell.* 2010;9(2):162-173. doi:10.1111/j.1474-9726.2009.00544.x
- 790 64. Blasco MA. Telomere length, stem cells and aging. *Nat Chem Biol.* 2007;3(10):640-649.
791 doi:10.1038/nchembio.2007.38
- 792 65. Bhattarai KR, Chaudhary M, Kim H-R, Chae H-J. Endoplasmic Reticulum (ER) Stress Response
793 Failure in Diseases. *Trends Cell Biol.* 2020;xx(xx):5-7. doi:10.1016/j.tcb.2020.05.004
- 794 66. De Leeuw CA, Neale BM, Heskes T, Posthuma D. The statistical properties of gene-set analysis.
795 *Nat Rev Genet.* 2016;17(6):353-364. doi:10.1038/nrg.2016.29
- 796 67. Loh PR, Bhatia G, Gusev A, et al. Contrasting genetic architectures of schizophrenia and other
797 complex diseases using fast variance-components analysis. *Nat Genet.* 2015;47(12):1385-1392.
798 doi:10.1038/ng.3431
- 799 68. Billingsley KJ, Barbosa IA, Bandrés-Ciga S, et al. Mitochondria function associated genes
800 contribute to Parkinson's Disease risk and later age at onset. *npj Park Dis.* 2019;5(1).
801 doi:10.1038/s41531-019-0080-x
- 802 69. Kraja AT, Liu C, Fetterman JL, et al. Associations of Mitochondrial and Nuclear Mitochondrial
803 Variants and Genes with Seven Metabolic Traits. *Am J Hum Genet.* 2019;104(1):112-138.
804 doi:10.1016/j.ajhg.2018.12.001
- 805 70. Jansen IE, Savage JE, Watanabe K, et al. Genome-wide meta-analysis identifies new loci and
806 functional pathways influencing Alzheimer's disease risk. *Nat Genet.* 2019;51(3):404-413.
807 doi:10.1038/s41588-018-0311-9
- 808 71. Pardiñas AF, Holmans P, Pocklington AJ, et al. Common schizophrenia alleles are enriched in
809 mutation-intolerant genes and in regions under strong background selection. *Nat Genet.*
810 2018;50(3):381-389. doi:10.1038/s41588-018-0059-2
- 811 72. Maurano MT, Humbert R, Rynes E, et al. Systematic localization of common disease-associated
812 variation in regulatory DNA. *Science (80-).* 2012;337(6099):1190-1195.
813 doi:10.1126/science.1222794
- 814 73. Raule N, Sevini F, Santoro A, Altilia S, Franceschi C. Association studies on human mitochondrial
815 DNA: Methodological aspects and results in the most common age-related diseases.
816 *Mitochondrion.* 2007;7(1-2):29-38. doi:10.1016/j.mito.2006.11.013
- 817 74. Yu X, Koczan D, Sulonen AM, et al. mtDNA nt13708A variant increases the risk of multiple
818 sclerosis. *PLoS One.* 2008;3(2):1-7. doi:10.1371/journal.pone.0001530
- 819 75. Hudson G, Nalls M, Evans JR, et al. Two-stage association study and meta-analysis of

- 820 mitochondrial DNA variants in Parkinson disease. *Neurology*. 2013;80(22):2042-2048.
821 doi:10.1212/WNL.0b013e318294b434
- 822 76. Samuels DC, Carothers AD, Horton R, Chinnery PF. The power to detect disease associations with
823 mitochondrial DNA haplogroups. *Am J Hum Genet*. 2006;78(4):713-720. doi:10.1086/502682
- 824 77. Biffi A, Anderson CD, Nalls MA, et al. Principal-Component Analysis for Assessment of Population
825 Stratification in Mitochondrial Medical Genetics. *Am J Hum Genet*. 2010;86(6):904-917.
826 doi:10.1016/j.ajhg.2010.05.005
- 827 78. Segrè A V, Consortium D, investigators M, et al. Common Inherited Variation in Mitochondrial
828 Genes Is Not Enriched for Associations with Type 2 Diabetes or Related Glycemic Traits. *PLoS*
829 *Genet*. 2010;6(8):e1001058. <https://doi.org/10.1371/journal.pgen.1001058>.
- 830 79. Saxena R, De Bakker PIW, Singer K, et al. Comprehensive association testing of common
831 mitochondrial DNA variation in metabolic disease. *Am J Hum Genet*. 2006;79(1):54-61.
832 doi:10.1086/504926
- 833 80. Hudson G, Gomez-Duran A, Wilson IJ, Chinnery PF. Recent Mitochondrial DNA Mutations
834 Increase the Risk of Developing Common Late-Onset Human Diseases. *PLoS Genet*. 2014;10(5).
835 doi:10.1371/journal.pgen.1004369
- 836 81. Hudson G, Panoutsopoulou K, Wilson I, et al. No evidence of an association between
837 mitochondrial DNA variants and osteoarthritis in 7393 cases and 5122 controls. *Ann Rheum Dis*.
838 2013;72(1):136-139. doi:10.1136/annrheumdis-2012-201932
- 839 82. Seidman JG, Seidman C. Transcription factor haploinsufficiency: When half a loaf is not enough. *J*
840 *Clin Invest*. 2002;109(4):451-455. doi:10.1172/JCI0215043
- 841 83. Lee R Van Der, Correard S, Wasserman WW. Deregulated Regulators : Disease-Causing cis
842 Variants in Transcription Factor Genes. *Trends Genet*. 2020;xx(xx). doi:10.1016/j.tig.2020.04.006
- 843 84. Arroyo JD, Jourdain AA, Calvo SE, et al. A Genome-wide CRISPR Death Screen Identifies Genes
844 Essential for Oxidative Phosphorylation. *Cell Metab*. 2016;24(6):875-885.
845 doi:10.1016/j.cmet.2016.08.017
- 846 85. Wright S. Physiological and Evolutionary Theories of Dominance. *Am Nat*. 1934;68(714):24.
- 847 86. Kacser H, Burns JA. The molecular basis of dominance. *Genetics*. 1981;97(3-4):639-666.
- 848 87. Chance B, Williams GR. RESPIRATORY ENZYMES IN OXIDATIVE PHOSPHORYLATION: III. THE
849 STEADY STATE. *J Biol Chem*. 1955;217(1):409-428. <http://www.jbc.org/content/217/1/409.short>.
- 850 88. Vafai SB, Mootha VK. Mitochondrial disorders as windows into an ancient organelle. *Nature*.
851 2012;491(7424):374-383. doi:10.1038/nature11707
- 852 89. Balaban RS, Kantor HL, Katz LA, Briggs RW. Relation between work and phosphate metabolite in
853 the in vivo paced mammalian heart. *Science (80-)*. 1986;232(4754):1121-1123.
854 doi:10.1126/science.3704638
- 855 90. To TL, Cuadros AM, Shah H, et al. A Compendium of Genetic Modifiers of Mitochondrial
856 Dysfunction Reveals Intra-organelle Buffering. *Cell*. 2019;179(5):1222-1238.e17.
857 doi:10.1016/j.cell.2019.10.032
- 858 91. Golan D, Lander ES, Rosset S. Measuring missing heritability: Inferring the contribution of
859 common variants. *Proc Natl Acad Sci U S A*. 2014;111(49):E5272-E5281.
860 doi:10.1073/pnas.1419064111
- 861 92. Polderman TJC, Benyamin B, De Leeuw CA, et al. Meta-analysis of the heritability of human traits
862 based on fifty years of twin studies. *Nat Genet*. 2015;47(7):702-709. doi:10.1038/ng.3285
- 863 93. Fuchsberger C, Flannick J, Teslovich TM, et al. The genetic architecture of type 2 diabetes.
864 *Nature*. 2016;536(7614):41-47. doi:10.1038/nature18642
- 865 94. Hill WG, Goddard ME, Visscher PM. Data and theory point to mainly additive genetic variance for
866 complex traits. *PLoS Genet*. 2008;4(2). doi:10.1371/journal.pgen.1000008
- 867 95. Zhu Z, Bakshi A, Vinkhuyzen AAE, et al. Dominance genetic variation contributes little to the

- 868 missing heritability for human complex traits. *Am J Hum Genet.* 2015;96(3):377-385.
869 doi:10.1016/j.ajhg.2015.01.001
- 870 96. Rand DM, Mossman JA. Mitonuclear conflict and cooperation govern the integration of
871 genotypes, phenotypes and environments. *Philos Trans R Soc B Biol Sci.* 2020;375(1790).
872 doi:10.1098/rstb.2019.0188
- 873 97. Sackton TB, Hartl DL. Genotypic Context and Epistasis in Individuals and Populations. *Cell.*
874 2016;166(2):279-287. doi:10.1016/j.cell.2016.06.047
- 875 98. Hemani G, Shakhbazov K, Westra HJ, et al. Detection and replication of epistasis influencing
876 transcription in humans. *Nature.* 2014;508(7495):249-253. doi:10.1038/nature13005
- 877 99. Solenski NJ, DiPierro CG, Trimmer PA, Kwan AL, Helms GA. Ultrastructural changes of neuronal
878 mitochondria after transient and permanent cerebral ischemia. *Stroke.* 2002;33(3):816-824.
879 doi:10.1161/hs0302.104541
- 880 100. Flameng W, Andres J, Ferdinande P, Mattheussen M, Van Belle H. Mitochondrial function in
881 myocardial stunning. *J Mol Cell Cardiol.* 1991;23(1):1-11. doi:10.1016/0022-2828(91)90034-J
- 882 101. Weinbrenner C, Liu GS, Downey JM, Cohen M V. Cyclosporine a limits myocardial infarct size
883 even when administered after onset of ischemia. *Cardiovasc Res.* 1998;38(3):676-684.
884 doi:10.1016/S0008-6363(98)00064-9
- 885 102. Kubben N, Misteli T. Shared molecular and cellular mechanisms of premature ageing and ageing-
886 associated diseases. *Nat Rev Mol Cell Biol.* 2017;18(10):595-609. doi:10.1038/nrm.2017.68
- 887 103. Garcia CK, Wright WE, Shay JW. Human diseases of telomerase dysfunction: Insights into tissue
888 aging. *Nucleic Acids Res.* 2007;35(22):7406-7416. doi:10.1093/nar/gkm644
- 889 104. Han S, Brunet A. Histone methylation makes its mark on longevity. *Trends Cell Biol.*
890 2012;22(1):42-49. doi:10.1016/j.tcb.2011.11.001
- 891 105. Bahar R, Hartmann CH, Rodriguez KA, et al. Increased cell-to-cell variation in gene expression in
892 ageing mouse heart. *Nature.* 2006;441(7096):1011-1014. doi:10.1038/nature04844
- 893 106. Kanfi Y, Naiman S, Amir G, et al. The sirtuin SIRT6 regulates lifespan in male mice. *Nature.*
894 2012;483(7388):218-221. doi:10.1038/nature10815
- 895 107. Karczewski KJ, Dudley JT, Kukurba KR, et al. Systematic functional regulatory assessment of
896 disease-associated variants. *Proc Natl Acad Sci U S A.* 2013;110(23):9607-9612.
897 doi:10.1073/pnas.1219099110
- 898 108. Purcell S, Neale B, Todd-Brown K, et al. PLINK: A tool set for whole-genome association and
899 population-based linkage analyses. *Am J Hum Genet.* 2007;81(3):559-575. doi:10.1086/519795
- 900 109. Yanai I, Benjamin H, Shmoish M, et al. Genome-wide midrange transcription profiles reveal
901 expression level relationships in human tissue specification. *Bioinformatics.* 2005;21(5):650-659.
902 doi:10.1093/bioinformatics/bti042
- 903 110. Melé M, Ferreira PG, Reverter F, et al. The human transcriptome across tissues and individuals.
904 *Science (80-).* 2015;348(6235):660-665. <http://dx.doi.org/10.1126/science.aaa0355>.
- 905 111. Morris JA, Randall JC, Maller JB, Barrett JC. Evoker: A visualization tool for genotype intensity
906 data. *Bioinformatics.* 2010;26(14):1786-1787. doi:10.1093/bioinformatics/btq280
- 907 112. Yates AD, Achuthan P, Akanni W, et al. Ensembl 2020. *Nucleic Acids Res.* 2020;48(D1):D682-D688.
908 doi:10.1093/nar/gkz966
- 909 113. Litman T, Stein WD. Obtaining estimates for the ages of all the protein-coding genes and most of
910 the ontology-identified noncoding genes of the human genome, assigned to 19 phylostrata.
911 *Semin Oncol.* 2019;46(1):3-9. doi:10.1053/j.seminoncol.2018.11.002
- 912 114. Orho-Melander M, Melander O, Guiducci C, et al. Common missense variant in the glucokinase
913 regulatory protein gene is associated with increased plasma triglyceride and C-reactive protein
914 but lower fasting glucose concentrations. *Diabetes.* 2008;57(11):3112-3121. doi:10.2337/db08-
915 0516

- 916 115. Krebs HA. The redox state of nicotinamide adenine dinucleotide in the cytoplasm and
917 mitochondria of rat liver. *Adv Enzyme Regul.* 1967;5(C):409-434. doi:10.1016/0065-
918 2571(67)90029-5
- 919 116. Goodman RP, Markhard AL, Shah H, et al. Hepatic NADH reductive stress underlies common
920 variation in metabolic traits. *Nature.* 2020;583(7814):122-126. doi:10.1038/s41586-020-2337-2
- 921 117. Howrigan D, Abbot L, Churchhouse C, Palmer DS. Details and considerations of the UK Biobank
922 GWAS. Neale lab blog. [http://www.nealelab.is/blog/2017/9/11/details-and-considerations-of-](http://www.nealelab.is/blog/2017/9/11/details-and-considerations-of-the-uk-biobank-gwas)
923 [the-uk-biobank-gwas](http://www.nealelab.is/blog/2017/9/11/details-and-considerations-of-the-uk-biobank-gwas). Published 2017.
- 924 118. Nguyen M, Wong YC, Ysselstein D, Severino A, Krainc D. Synaptic, Mitochondrial, and Lysosomal
925 Dysfunction in Parkinson's Disease. *Trends Neurosci.* 2019;42(2):140-149.
926 doi:10.1016/j.tins.2018.11.001
- 927 119. Grünewald A, Kumar KR, Sue CM. New insights into the complex role of mitochondria in
928 Parkinson's disease. *Prog Neurobiol.* 2019;177(April 2018):73-93.
929 doi:10.1016/j.pneurobio.2018.09.003
- 930 120. Abou-Sleiman PM, Muqit MMK, Wood NW. Expanding insights of mitochondrial dysfunction in
931 Parkinson's disease. *Nat Rev Neurosci.* 2006;7(3):207-219. doi:10.1038/nrn1868
- 932 121. Ge P, Dawson VL, Dawson TM. PINK1 and Parkin mitochondrial quality control: A source of
933 regional vulnerability in Parkinson's disease. *Mol Neurodegener.* 2020;15(1):1-18.
934 doi:10.1186/s13024-020-00367-7
- 935 122. Bose A, Beal MF. Mitochondrial dysfunction in Parkinson's disease. *J Neurochem.* 2016;139:216-
936 231. doi:10.1111/jnc.13731
- 937 123. Müller-Nedebock AC, Brennan RR, Venter M, et al. The unresolved role of mitochondrial DNA in
938 Parkinson's disease: An overview of published studies, their limitations, and future prospects.
939 *Neurochem Int.* 2019;129(April):104495. doi:10.1016/j.neuint.2019.104495
940